ADVANCED FUNCTIONAL MATERIALS
www.afm-journal.de

Highly Fluorescent Thienoviologen-Based Polymer Gels for Single Layer Electrofluorochromic Devices

Amerigo Beneduci, Sante Cospito, Massimo La Deda, and Giuseppe Chidichimo*

A highly fluorescent electrofluorochromic gel with quantum yields as high as 67% is prepared by incorporating the thienoviologen fluorophore 4,4′-(2,2′-bithiophene-5,5′-diyl)*bis*(1-nonylpridinium)bistriflimide into a polymeric matrix. The fluorescent emission spectrum of the gel at low percentages of thienoviologen shows a strong band at 530 nm. A new intense fluorescence band at 630 nm can be induced by fluorophore aggregation. Single layer electrofluorochromic devices were readily prepared by sandwiching the polymer gels between two indium tin oxide (ITO) electrodes. The fluorescence intensity can be easily modulated between a fluorescent and a quenched state, in a wide visible spectral range, by direct electrochemical reduction of the thienoviologen fluorophore. It exhibits three reduction states, each with different emission properties. The reversible interconversion among these states leads to a high electrofluorochromic stability of the device, exhibiting switching times of a few seconds and, to the best of our knowledge, the highest contrast ratio (337).

1. Introduction

Fluorescent materials in which their photoluminescence can be modulated by external stimuli have attracted increasing interest because of their wide range of applications in the UV–vis spectral range as sensors,[1] optical and electronic devices,[2] fluorescence imaging,[3] and memory and displays[4] as well as in the near-infrared (NIR) region[5] concerning applications in bioimaging,[6] bioanalysis,[7] and night vision devices.[8] A promising approach to provide reversible and stable fluorescence modulation is based on the conversion of the redox states of a material by electrochemical reactions and is known as electrofluorochromism.[4,5] Common electrofluorochromic (EFC) materials include molecular dyads,[4d,5b,9] conjugated polymers,[2e,10] and small molecules acting as intrinsically switchable fluorophores.[4a,c,11] In principle, the last ones are the most attractive since their fluorescence can be simply switched by direct electrochemical conversion to the corresponding radical-ion. In addition, compared to dyads and polymers, they have well defined molecular structure and weight for convenient synthesis and purification. Unfortunately, most of the ion-radicals formed from these fluorophores are not fluorescent or are unstable and their fluorescence can be hardly monitored;[4e] in such a case, irreversible electrofluorescence switch could arise.

Recently, we presented a new class of intrinsically switchable fluorophores, the thienoviologens dications 4,4′-(2,2′-bithiophene-5,5′-diyl)*bis*(1-alkylpridinium) (TV^{++}). Their electrochemical reduction leads to direct fluorescence switching in the bulk liquid crystalline phases above 100 °C.[11a] However, the high operational temperatures required, hamper their direct application in room-temperature devices. Here we show that, the strong fluorescence thienoviologens, can be advantageously used in single layer ITO/EFC/ITO devices, in which the EFC layer was a polymer gel containing the fluorophore, simply drop-casted onto one ITO electrode. The EFC layer was formed with polyvinyl formal (PVF), *N*-methyl-2-pyrrolidone (NMP) solvent, the thienoviologen fluorophore 4,4′-(2,2′-bithiophene-5,5′-diyl)*bis*(1-nonylpridinium)bistriflimide ($TV[NTf_2]_2$), and ferrocene (**Figure 1**). NMP was chosen because it is a good solvent for all the gel components, is transparent in the UV–vis spectral range and is a good plasticizer for the polymer PVF.[12] It has also the advantage of having a high-boiling point (202 °C) so that no evaporation of this component occurs during the thermal blending process above the glass transition temperature of the polymer (T_g = 108 °C). Moreover,

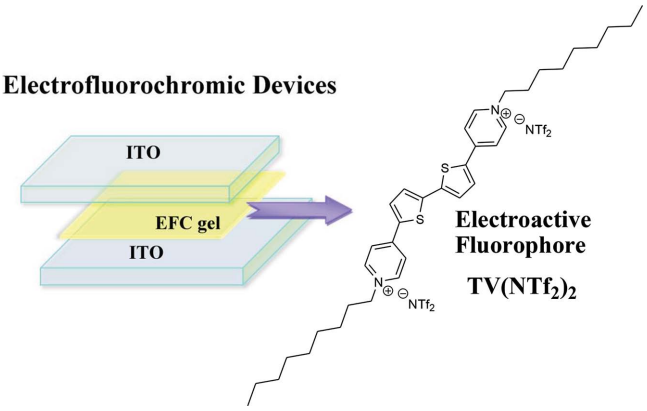

Figure 1. Single layer ITO/EFC gel/ITO device. The active electrofluorochromic layer contains the highly fluorescent intrinsically switchable fluorophore thienoviologen 4,4′-(2,2′-bithiophene-5,5′-diyl)*bis*(1-nonylpridinium)bistriflimide $TV(NTf_2)_2$.

Dr. A. Beneduci, Dr. S. Cospito, Dr. M. La Deda, Prof. G. Chidichimo
Department of Chemistry and Chemical Technology
University of Calabria
Via Pietro Bucci, Cubo 15C, 87036 Arcavacata di Rende (CS), Italy
E-mail: amerigo.beneduci@unical.it

DOI: 10.1002/adfm.201403611

PVF has excellent adhesive performances on glass and many other substrates.[12b,13a,b] Indeed, the resulting gel was self-supporting and remained firmly glued on the ITO surfaces of the device at room temperature even when the cell was subjected to strong mechanical stresses. Ferrocene was used as anodic complementary component,[12a,13] in order to improve device performances in terms of fluorescence contrast, response times, and reversibility.

The EFC devices presented here exhibit high fluorescence contrast ratios and short switching times in a wide range of the visible spectrum. Such performances are retained for more than 90% even after long-time scale working operation up to 500 switching cycles.

2. Results and Discussion

2.1. Electrochemistry of the Device

The cyclic voltammetry (CV) of the gel was measured with a pseudo ITO/EFC gel/ITO three-electrode cell in which two ITO plates served as working and counter electrodes and the Ferrocenium/Ferrocene couple, contained in the gel, was used as reference internal standard (**Figure 2**).

The CV diagram reported in Figure 2a shows three redox processes at half wave potentials of +0.082, −1.12, and −1.34 V, respectively related to the Fc^+/Fc couple, to the reduction of the thienoviologen dication (TV^{++}) into the radical-cation ($TV^{\cdot+}$), and to the reduction of the $TV^{\cdot+}$ species into the neutral one (TV) (Figure 2b; scheme I). The cathodic to anodic peak ratio (i_{pc}/i_{pa}) for ferrocene and for the first redox couple of the thienoviologen ($TV^{++}/TV^{\cdot+}$) is close to unity. In contrast, the i_{pc}/i_{pa} for the second redox process of thienoviologen is larger than unity. The neutral species is a powerful reducing agent,[14] and can react with Fc^+ (cycle II) and, in a comproportionation reaction with the dication TV^{++} (cycle III), frequently observed in bypiridinium systems,[14a,d] to form the radical cation. At di-reduction potentials, the processes occurring close to the cathode and at the forefront between the cathode and the bulk, are depicted in Figure 2b and involve the following steps: electro-formation of the direduced TV (Equation (1); Figure 2, scheme II); comproportionation reaction (Equation (2); Figure 2, scheme III); chemical reaction with Fc^+ (Equation (3);

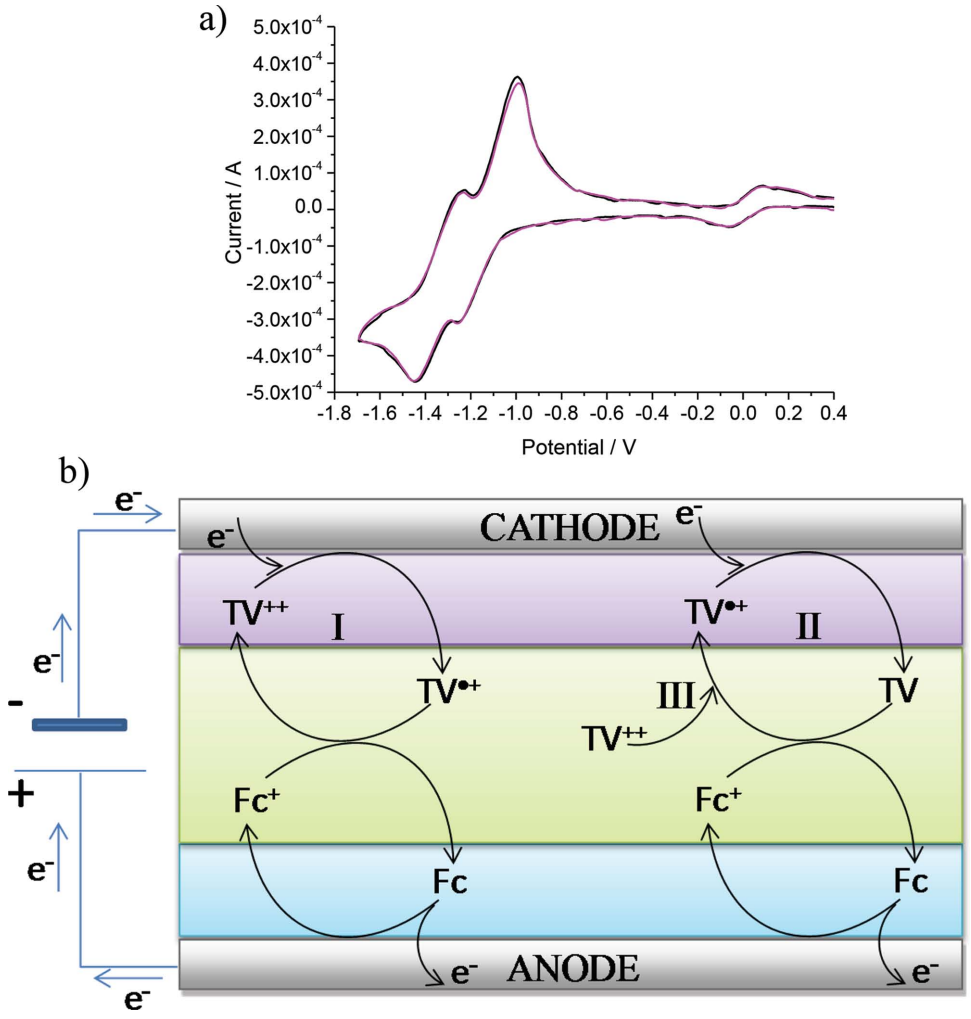

Figure 2. a) Cyclic voltammetry of the gel recorded on a 2.5 × 1.8 cm^2 electrode surface at 20 mV s^{-1} for the first cycle (black curve) and after 50 CV cycles (magenta curve). b) Scheme of the electrochemical working mechanism of the EFC device.

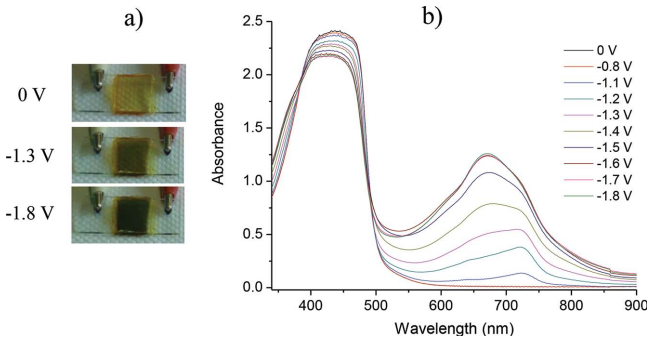

Figure 3. Absorption spectra of the gel sandwiched between two-ITO electrodes (cell gap of 7 μm) as a function of the potential.

Figure 2, scheme II); and then electro-formation of the direduced TV [Equation (1)].

$$TV^{\bullet+} + 1e^- = TV \quad (1)$$

$$TV + TV^{++} = 2TV^{\bullet+} \quad (2)$$

$$TV + Fc^+ = TV^{\bullet+} + Fc \quad (3)$$

If the chemical reactions (2) and (3) (at least one of them) occur with fast kinetics, the concentration of the neutral species becomes low with respect to the radical-cation. Under these conditions, a high i_{pc}/i_{pa} for the $TV^{\bullet+}/TV$ couple should be expected since this ratio is proportional to the $\frac{[TV^{\bullet+}]}{[TV]}$ concentration ratio. Nevertheless, since reaction (2) and (3) regenerates the radical-cation, the overall electrochemical process is reversible, as indicated by the i_{pc}/i_{pa} close to unity for the first redox couple.

At increasing scan rates, the behavior is similar, i.e., the i_{pc}/i_{pa} for the $TV^{++}/TV^{\bullet+}$ couple is still close to unity, while the i_{pc}/i_{pa} for the $TV^{\bullet+}/TV$ couple is larger than unity, (Figure S1, Supporting Information). Reversibility is further supported by a very slight dependence of the peaks potential on the scan rate (Figure S1, Supporting Information)

The scheme in Figure 2b also illustrates the other electrochemical processes occurring in the bulk where the mono-reduced species ($TV^{\bullet+}$) reacts with the Fc^+ ion to form ferrocene, and at the anode in which the ferrocene acts as anodic component and delivers electrons to the anode, where it is oxidized to ferrocenium.

2.2. Absorption Spectroelectrochemistry of the EFC Gels

The formation of the reduced species is accompanied by a color change of the gel from yellow to deep green (**Figure 3**a). This typical electrochromic response was studied by spectroelectrochemical investigation performed on a thin film of the gel (Figure 3b). The off-state optical spectrum is characterized by the strong absorption band at 430 nm due to the $\pi \rightarrow \pi^*$ transition typical of the TV^{++} species.[15] Reduction to the radical-cation gives rise to a new absorption band in the 530–880 nm range that grows up with increasing negative voltages. As can be seen in Figure 3a, a more intense color of the same hue is observed following direduction and this corresponds to an increase of the electrochromic absorption band (Figure 3b). The neutral species of bipyridinium systems is generally weakly colored. Thus, the electrochromic band is still due to the radical cation that is generated during the comproportionation reaction [Equation (2)] or during reaction with ferrocenium ion [Equation (3)].

2.3. Emission Spectroelectrochemistry of the EFC Gels

Figure 4 displays the fluorescent emission spectra of the EFC gel as a function of the percentage of thienoviologen. At 2% (w/w), the spectrum is very similar to that in dilute solutions,[11a] showing an emission band centered at 530 nm. As the percentage of thienoviologen increases, an additional emission band at λ_{max} = 630 nm gradually grows up until,

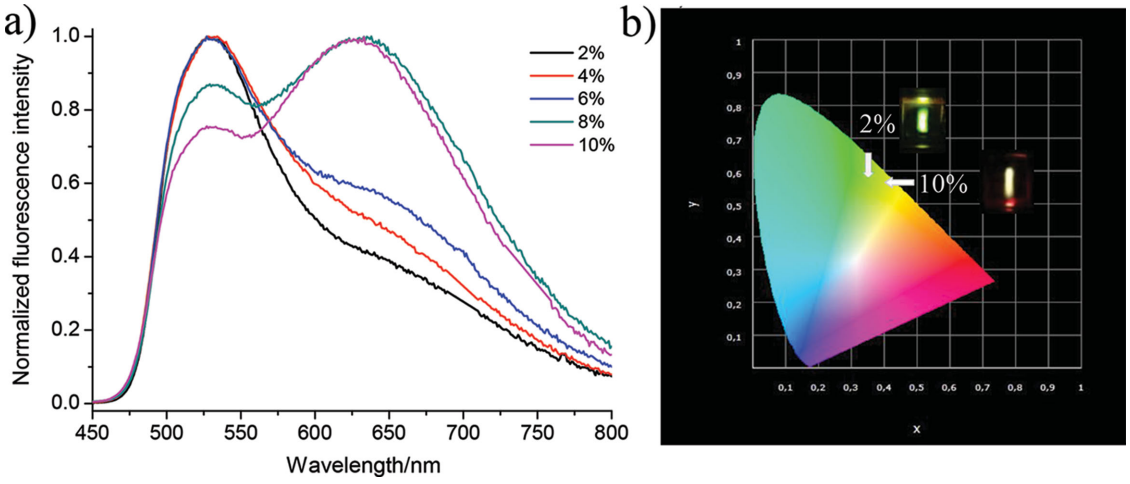

Figure 4. a) Dependence of the fluorescence spectrum of the EFC gel on the percentage of thienoviologen. b) CIE XY diagram of the fluorescence of the gel with 2% and 10% of thienoviologen.

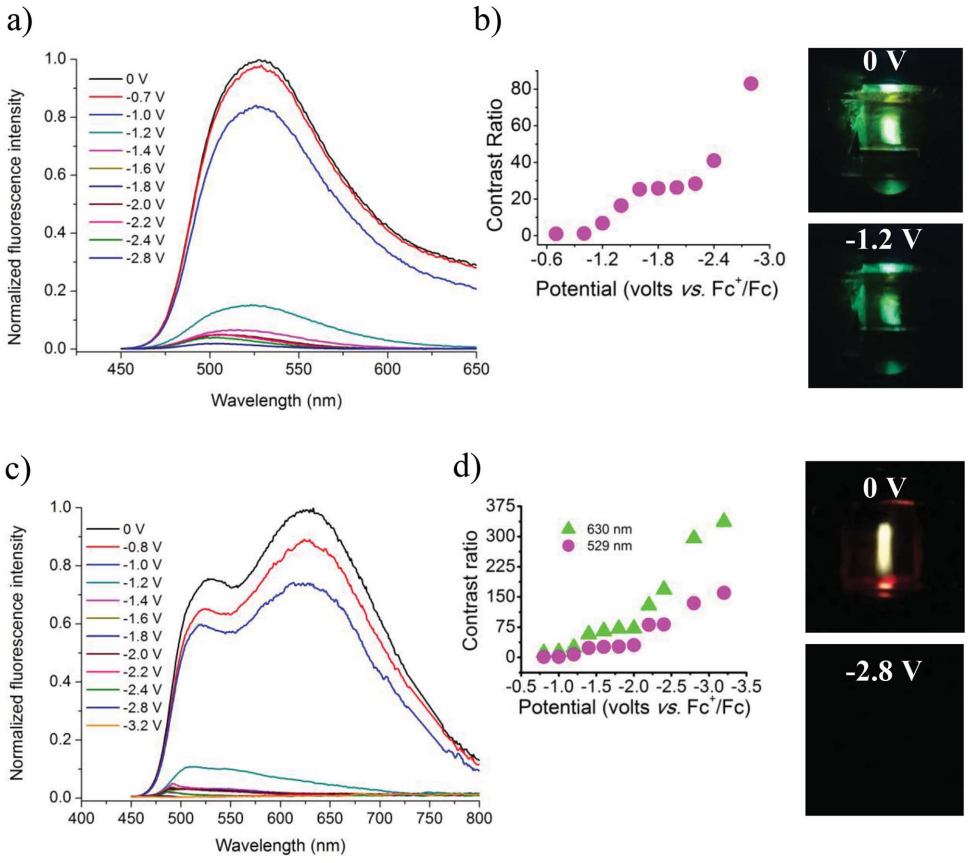

Figure 5. Electrofluorescence properties of the gels. a) Fluorescence spectra as a function of the applied voltage for the gel with 2% (w/w) of thienoviologen. Each spectrum was acquired after 40 s of application of the target potential. b) Fluorescence contrast ratio at 530 nm as a function of the applied voltage. c) Fluorescence spectra as a function of the applied voltage of the gel with 10% (w/w) of thienoviologen. Each spectrum was acquired after 40 s of application of the target potential. d) Fluorescence contrast ratio at 630 and 529 nm as a function of the applied voltage. The photos on the right show the fluorescence of the devices with 2% (up right) and 10% (down right) of $(TV(NTf_2)_2$ (λ_{ex} = 370 nm) under different applied voltages.

above 6%, it dominates the fluorescence spectrum (Figure 4a). This band is determined by the aggregation of the thienoviologen in solution, which occurs at concentrations as low as 10^{-3}M.[11a] The aggregates are sufficiently stable to be preserved during the mixing step with the polymer at 120 °C, needed for preparing the EFC gel.

The overall fluorescence color of the gel changes as a function of the thienoviologen percentage, as can be clearly seen in Figure 4b, where representative photos of the fluorescence emissions of the gels with 2% and 10% of thienoviologen are reported on the C.I.E. (Commission Internationale de l'Eclairage) chromaticity diagram (Figure 4b).

Some photophysical properties of the gels are reported in Table S1 (Supporting Information), where it can be seen that they exhibit extremely high quantum yields (up to 67%).

The response of the fluorescence to the application of dc reductive voltages, in the case of the gel at 2% of $TV(NTf_2)_2$, is shown in **Figure 5**a. A fluorescence quenching was observed just at negative potentials close to the first reduction of the thienoviologen dication. Under these conditions, the radical-cation species is formed which, as previously shown, is highly emissive.[11a] In order to explain the observed quenching, an energy transfer mechanism can come into play in this case, as can be inferred by the overlap between the emission spectrum of the TV^{++} species and the absorption spectrum of the radical-cation (Figure S2, Supporting Information).[2e,4e,9b,c,e,11b,c,16]

When complete electrochemical reduction to the neutral thienoviologen species is achieved, the fluorescence quenching becomes relevant. In these conditions, a contribution to the quenching may derive from the formation of the neutral species that, as previously shown, is not emissive.[11a]

The fluorescence intensity drop coincides with a steep increase of the fluorescence contrast ratio (Figure 5b). This is defined as the ratio between the intensity maximum in the off-state (i_{off}) and in the on-state spectrum (i_{on}).[2e,10] Based on this definition, values of i_{off}/i_{on} as high as 83 were obtained at –2.8 V after 40 s of potential application (Figure 5b). However, this definition does not take into account for the intensity changes across the whole fluorescence emission band. For this reason, a more appropriate metric for this parameter may be the ratio between the emission spectral areas in the off and on states. The values of the contrast ratio calculated in this way are reported in Figure S3 (Supporting Information).

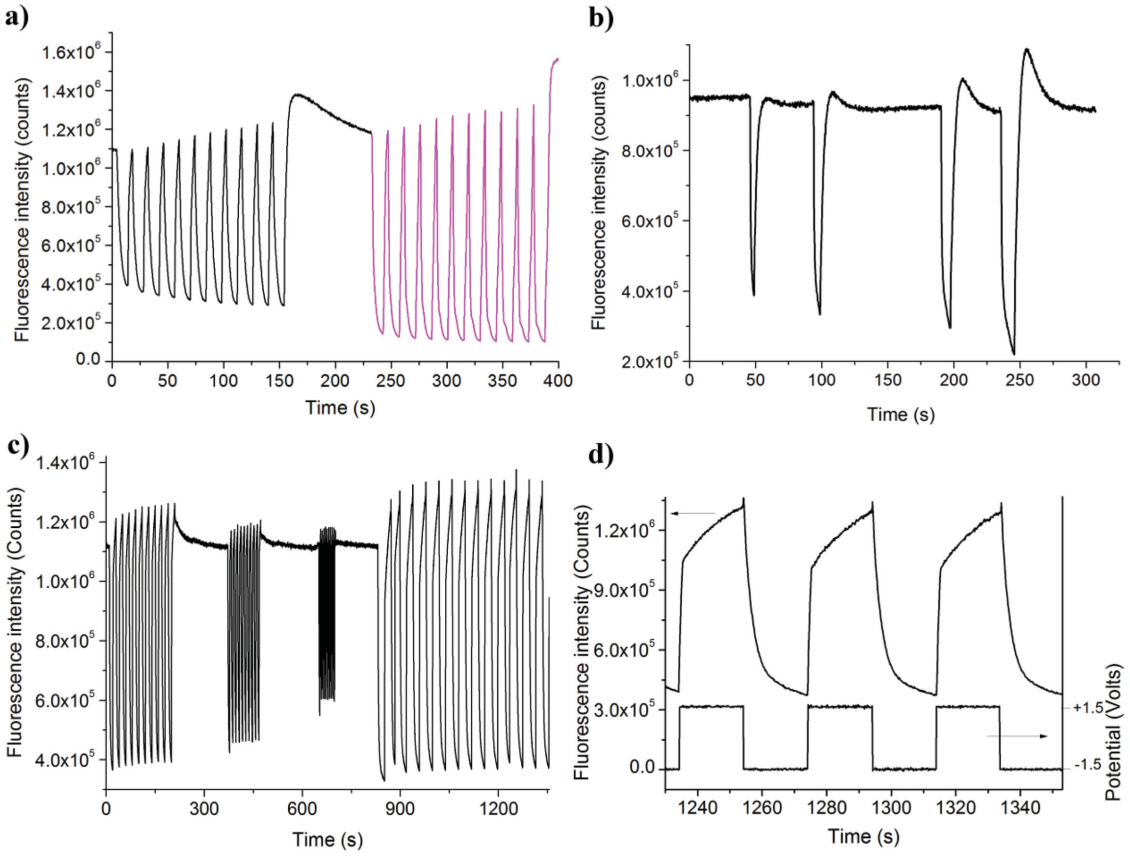

Figure 6. Electrofluorescence switching achieved with repetitive square-wave potentials at a) 690 nm between −1.2 V for 10 s and 0 V for 4 s (black curve) and −1.5 V for 10 s and 0 V for 4.5 s (magenta curve); b) −1.5 and 0 V for 3, 5, 7, and 10 s, respectively; c) at 530 nm between −1.5 and +1.5 V for 10 s, 5 , 2.5, and 20 s, respectively. d) Zoom of the last sequence of c) showing the details of the square wave fluorescence response. The time resolution was 156 ms for all experiments.

The fluorescence response of the aggregates to the electrochemical reduction is reported in the spectral sequence of Figure 5c. As can be seen, it is similar to that of the single species, leading to a progressive quenching of the high wavelength fluorescence band. In such a case, the contrasts measured at 630 nm were higher than those measured at 530 nm, for equal applied potentials and step duration. Superb contrast ratios (i_{off}/i_{on}) of up to 337 and 135 were obtained at −3.2 V, respectively at 630 and 530 nm (Figure 5d). The energy-transfer mechanism[2e,4e,9b,c,e,11b,c,16] should be more relevant in the presence of the aggregates, due to the larger spectral overlap (Figure S2, Supporting Information), and this could be responsible of the higher contrast ratio observed in this case.

The overall fluorescence emission can be almost totally quenched at −2.8 V (photos in Figure 5). This occurs just after a few seconds, as shown in Movie S1 (Supporting Information), where the fluorescence of a ITO cell containing the EFC gel with 10% of thienoviologen, was monitored under 350 nm light source excitation during the application of repetitive on/off switching cycles between −2.8 and + 2.8 V.

It is worth highlighting here that, by changing the percentage of the fluorophore in the gel, it is possible to efficiently achieve fluorescence intensity modulation on a large portion of the visible spectrum, in the 470–800 nm range.

2.4. Electrofluorescence Switching

Some interesting features, that shed light into the electrofluorochromic mechanism, comes from the electrofluorescence switching study (**Figure 6**). The first sequence reported in Figure 6a was collected by applying a dc square wave potential between −1.2 V for 10 s and 0 V for 4 s and monitoring the fluorescence intensity at 690 nm. It can be seen that the square wave fluorescence response is amplified at each cycle because peak maximum and minimum increases and decreases, respectively. The average contrast ratio and switching times are reported in **Table 1**. After the last switching cycle, when the system is left at zero voltage, the fluorescence reaches an absolute maximum and then it decays back to its starting value. The above pattern could be qualitatively explained by considering the accumulation of the dication at the cathode, at each cycle, which has not enough time to diffuse into the bulk during the positive switch. It is important to highlight that the fluorescence measurements were done in a front-face geometry with the cathode chosen to be the illuminated electrode. Under these conditions, the fluorescence signal was mostly due to the layers of the material closer to the cathode. Therefore, this accumulation results in an increase of the fluorescence contrast at each cycle. Indeed, by inverting the potential sign in order to have the anode illuminated, modest quenching was observed. The last cycle nicely

Table 1. Electrofluorescence performances of the devices.

Switching pulses reported in Figure 6		i_{off}/i_{on}	ΔFL%[a)]	τ_{on} [s][b)]	τ_{off} [s][b)]
a	1st sequence	3.7 (0.5)	72.5 (4.3)	4.9 (0.6)	3.3 (0.8)
	2nd sequence	11.3 (1.4)	91.0 (1.2)	3.0 (0.8)	3.7 (0.4)
	b	2.5 (0.1)	59.4 (0.4)	1.7 (0.3)	3.3 (0.4)
		2.8 (0.2)	64.6 (0.5)	2.7 (0.2)	3.7 (0.3)
		3.2 (0.2)	68.3 (0.4)	3.9 (0.3)	3.7 (0.2)
		4.1 (0.3)	75.9 (0.5)	5.6 (0.4)	5.5 (0.3)
	c	3.19 (0.05)	68.7 (0.5)	5.2 (0.3)	3.8 (0.4)
		2.57 (0.03)	61.1 (0.4)	3.6 (0.1)	1.2 (0.1)
		1.96 (0.03)	49.0 (0.9)	1.9 (0.2)	0.781 (0.002)
		3.6 (0.1)	73.1 (3.6)	7.2 (0.6)	11.0 (3.3)

All the values are the mean (s.d.) over 15 switching cycles. [a)]The fluorescent contrast (ΔFL%) is defined as the difference between the fluorescence intensity in the on and off states; [b)]The switching time was defined as the time required for reach 90% of the full change in fluorescence (ΔFL) after the switching of the potential.

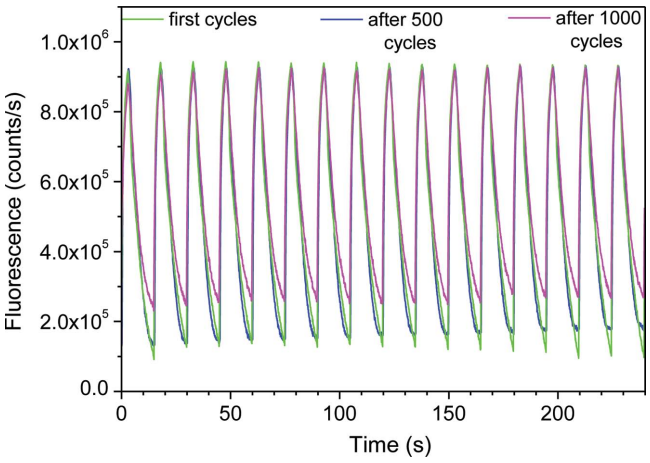

Figure 7. Electrofluorescence switching at 530 nm between −1.8 V for 10 s and 0 V for 5 s in the first cycles (green curve), after 500 cycles (blue curve) and after 1000 cycles (magenta curve).

shows the reversibility of the process since, when the potential is switched off, the reduced species is completely reoxidized to the dication producing the absolute maximum of fluorescence intensity. The dication then diffuses into the gel bulk in a time range dependent on the switching pulse conditions and number of cycles (e.g., in Figure 6a, it took about 90 s), causing the fluorescence to relax back to its original value.

A similar trend was also found at potentials for which the second reduction of the thienoviologen takes place, producing the nonemissive TV species (Figure 6a, magenta curve). Under these conditions, an increase of the contrast ratio was observed probably due to: a) the formation of the nonemissive neutral species and b) to a more efficient energy transfer mechanism caused by an increased electrochromic response (Figure S2, Supporting Information).

The effect of the negative pulse length on the electrofluorescence switching is shown in Figure 6b. Each pulse was performed at −1.5 V and the delay time between pulses at 0 V was large enough to allow complete relaxation. Each electrofluorescence cycle is similar to the last cycle in Figure 6a, with an intensity maximum occurring in the positive return sweep cycle. Both, fluorescence contrast and fluorescence maximum, increase with the negative pulse length (Table 1).

Highly repetitive electrofluorescence switching patterns can be obtained by the application of consecutive complete sweep cycles between negative and positive voltages with the same pulse length (Figure 6c). In such a case, the accumulation of the dication species occurs mainly in the first cycle after which no significant signal amplification was observed because its direct electrochemical oxidation occurs at the anode (former the cathode) due to potential inversion. Interestingly, the fine structure of the EFC switching reveals that, at each potential inversion from positive to negative values, a fluorescence spike systematically appears (Figure 6d). This could reflect the high emission of the radical-cation, whose instantaneous formation at the cathode, could be detected before any fluorescence quenching process takes place.

We have also investigated the stability of the device with 2% of $TV(NTf_2)_2$. As it can be seen in **Figure 7**, the device was cycled between −1.8 V for 10 s and 0 V for 5 s up to 1000 cycles (15 000 s). The reversibility of the device is excellent up to about 500 cycles after which the contrast ratio decreases from 6.1 (0.1) in the first cycles to 5.46 (0.06), corresponding to an EFC stability of more than 90%. A good stability (65%) is still retained up to 1000 cycles with a decrease of the contrast ratio to 4.0 (0.1).

3. Conclusions

In conclusion, here we showed an electrofluorochromic polymer gel based on the intrinsically switchable fluorophore thienoviologen. The emission properties of the EFC gels depend on the fluorophore percentage: in the 2%–6% (w/w) range the spectrum is dominated by the emission band centered at 530 nm. Above this concentration range, a new band adds at 630 nm arising from the formation of thienoviologen aggregates.

The very high fluorescence quantum yield of the gels can be efficiently quenched by direct electrochemical reduction of the fluorophore, giving rise to the highest contrast ratio reported so far. This process was used to modulate the fluorescence intensity between a highly emissive off state and a low emissive on state. Electrofluorescence switching was achieved over a wide visible spectral region from 470 up to 800 nm.

The electrofluorochromic gel was used to build up a single layer ITO/EFC gel/ITO device that, in contrast to multilayer EFC devices requiring several preparation steps for their assembling,[2e,9c,10,16] it is easily prepared in one step by drop casting and sandwiching. In addition, the gel is self-supporting due to their gluing action on ITO glass and can, in principle, be easily processed by extrusion or moulding in any desirable form. Moreover, by modifying the concentration of the fluorophore in the gel, various colors of the emitted light are achievable. These valuable features represent interesting technological solutions for practical applications.

4. Experimental Section

Materials: 4,4′-(2,2′-bithiophene-5,5′-diyl)*bis*(1-nonylpridinium) triflimide ($TV(NTf_2)_2$) was synthesized freshly before use, as previously reported.[17] The EFC polymer gels were prepared at different $TV(NTf_2)_2$ percentages from 2% up to 10% (w/w), above which solubility problems arise. The other components of the mixtures were ferrocene (Sigma-Aldrich) (0.3%–1.7% (w/w)), (PVF, Sigma-Aldrich) (35% (w/w)) and anhydrous *N*-methyl-2-pyrrolidinone, (NMP, Pancreac) (62.7%–53.3% (w/w)). In order to obtain high reproducibility in the fluorescent emission spectrum of the gels, the $TV(NTf_2)_2$ and ferrocene powders were first dissolved in NMP at room temperature and then mixed with the polymer under continuous stirring at 120 °C for 30 min.

EFC Device Preparation: ITO/EFC gel/ITO devices were assembled by drop casting the hot EFC mixture onto a ITO-coated glass support (Visiontek Systems Ltd. with a sheet resistance of 25 Ω sq^{-1} and a thickness of 1 mm) with a second ITO electrode used to create a sandwich with active area of about 1.5 × 1.0 cm^2. The cell thickness was controlled by inserting cylindrical spacers with mean base diameter of 5 × 10^{-6} m. The final cell gap was calculated by the interference fringes in its absorption spectrum in the NIR spectroscopy range (900–1500 nm).

Measurements: Standard cyclic voltammetry of the electrofluorochromic polymer gel (EFC gel) was performed with an Amel Instruments 7050 model potentiostat on an ITO/ EFC gel/ITO cell in which the two ITO plates served as working and counter electrodes and the Ferrocenium/Ferrocene redox couple as third pseudo-standard electrode. DC square wave voltages for the electrofluorescence switching study were supplied by an Amel 2049 model potentiostat connected to an Amel 568 model programmable function generator. The photophysical investigations in solution were performed with spectrofluorimetric grade solvents. The absorption spectra were acquired with Perkin Elmer Lambda 900 spectrophotometer. Steady-state emission spectra were recorded on a HORIBA Jobin–Yvon Fluorolog-3 FL3–211 spectrometer equipped with a 450 W xenon arc lamp, double-grating excitation and single-grating emission monochromators (2.1 nm mm^{-1} dispersion; 1200 grooves mm^{-1}), and a Hamamatsu R928 photomultiplier tube. Emission and excitation spectra were corrected for source intensity (lamp and grating) and emission spectral response (detector and grating) by standard correction curves. Time-resolved measurements were performed using the time-correlated single-photon counting option on the Fluorolog 3. The sample was excited with a Laser Nanoled at 379 nm and fwhm 750 ps, with repetition rate at 1 MHz. Excitation sources were mounted directly on the sample chamber at 90° to a single-grating emission monochromator (2.1 nm mm^{-1} dispersion; 1200 grooves mm^{-1}) and collected with a TBX-04-D single-photon-counting detector. The photons collected at the detector are correlated by a time-to-amplitude converter to the excitation pulse. Signals were collected using an IBH Data Station Hub photon counting module. The commercially available DAS6 software (HORIBA Jobin–Yvon IBH) was used for data analysis. Goodness of fit was assessed by minimizing the reduced Chi squared function (χ^2) and visual inspection of the weighted residuals. The emission quantum yields of the samples were obtained by means of a Labsphere optical Spectralon® integrating sphere (diameter 102 mm), which provides a reflectance >99% over 400–1500 nm range (>95% within 250–2500 nm). The sphere accessories are made from Teflon (rod and sample holders) or Spectralon (baffle). The sphere is mounted in the optical path of the spectrofluorimeter using, as excitation source, a 450 W Xenon lamp coupled with a double-grating monochromator for selecting wavelengths. Cylindrical tubes containing the solution samples are placed into the sphere, while the ITO sandwich, containing the sample, is placed into the sphere on a customized temperature-controlled hot stage realized in Teflon by CaLCTec s.r.l. (Rende, Italy), with an uncertainty on the temperature of 1 °C. The procedure used to determine the emission quantum yield is based on the de Mello method[18a] slightly modified.[18b,c] The emission quantum yield was calculated by Equations (4) and (5)

$$\Phi_F = \frac{\left(E_c - (1-A)E_a\right)}{L_a A} \tag{4}$$

where A is the value of the absorbance of the sample at the excitation wavelength measured as

$$A = \frac{\left(L_a - L_c\right)}{L_a} \tag{5}$$

where L_a is the integrated excitation profile when the reference sample is diffusely illuminated by the integrated sphere's surface; L_c is the integrated excitation profile when the sample is diffusely illuminated by the integrated sphere's surface; E_c and E_a are the integrated luminescence (corrected for the detector wavelength response) of the sample and the reference sample, respectively, caused by indirect illumination from the sphere. The reference sample is an empty quartz sandwich. The experimental uncertainties were 1 nm for the band maxima of the luminescence spectra and 5% for the emission quantum yield values.

Supporting Information

Supporting Information is available from the Wiley Online Library or from the author.

Acknowledgements

The authors thank the University of Calabria. This work is co-funded by the European Commission, the European Social Fund and by the Regione Calabria. The authors are the unique responsible of this work and both the European Commission and the Regione Calabria refuse any responsibility on the use of the information reported here. The authors are gratefully to Dr. Vito Maltese for the synthesis of the thienoviologen.

Received: October 15, 2014
Published online: December 16, 2014

[1] a) M. H. Lee, Z. G. Yang, C. W. Lim, Y. H. Lee, S. D. Bang, C. H. Kang, J. S. Kim, *Chem. Rev.* **2013**, *113*, 5071; b) B. Wang, R. Q. Meng, L. H. Bi, L. X. Wu, *Dalton Trans.* **2011**, *40*, 5298; c) T. Li, M. Famulok, *J. Am. Chem. Soc.*, **2013**, *135*, 1593.

[2] a) P. Belser, L. D. Cola, F. Hartl, V. Adamo, B. Bozic, Y. Chriqui, V. M. Iyer, R. T. F. Jukes, J. Kuhni, M. Querol, S. Roma, N. Salluce, *Adv. Funct. Mater.* **2006**, *16*, 195; b) H. L. Li, S. P. Pang, S. Wu, X. L. Feng, K. Müllen, C. Bubeck, *J. Am. Chem. Soc.* **2011**, *133*, 9423; c) G. Liu, S. Z. Pu, R. J. Wang, *Org. Lett.*, **2013**, *15*, 980; d) F. M. Raymo, M. Tomasulo, *Chem. Soc. Rev.* **2005**, *34*, 327; e) C. P. Kuo, C. N. Chuang, C. L. Chang, M. K. Leung, H. Y. Lianc, K. C. W. Wu, *J. Mater. Chem. C.* **2013**, *1*, 2121.

[3] a) I. Yildiz, E. Deniz, F. M. Raymo, *Chem. Soc. Rev.* **2009**, *38*, 1859; b) C. L. Yeung, P. Iqbal, M. Allan, M. Lashkor, J. A. Preece, P. M. Mendes, *Adv. Funct. Mater.* **2010**, *20*, 2657; c) G. Ding, H. Zhou, J. Xu, X. Lu, *Chem. Commun.* **2014**, *50*, 655.

[4] a) Y. Kim, E. Kim, G. Clavier, P. Audebert, *Chem. Commun.* **2006**, *34*, 3612; b) Y. S. Zhao, H. B. Fu, A. D. Peng, W. S. Yang, J. N. Yao, *Adv. Mater.* **2008**, *20*, 79; c) Y. Kim, J. Do, E. Kim, G. Clavier, L. Galmiche, P. Audebert, *J. Electroanal. Chem.* **2009**, *632*, 201; d) F. Miomandre, J. F. Audibert, Q. Zhou, P. Audebert, P. Martin, J. C. Lacroix, *Electrochim. Acta* **2013**, *110*, 56; e) P. Audebert, F. Miomandre, *Chem. Sci.* **2013**, *4*, 575.

[5] a) S. Seo, S. Pascal, C. Park, K. Shin, X. Yang, O. Maury, B. D. Sarwade, C. Andraud, E. Kim, *Chem. Sci.* **2014**, *5*, 1538;

b) N. L. Bill, J. M. Lim, C. M. Davis, S. Bähring, J. O. Jeppesen, D. Kim, J. L. Sessler, *Chem. Commun.* **2014**, *50*, 6758; c) X. Cheng, Z. Zhang, H. Zhang, S. Han, K. Ye, L. Wang, H. Zhang, Y. Wang, *J. Mater. Chem. C* **2014**, *2*, 7385.

[6] a) S. Kim, Y. T. Lim, E. G. Soltesz, A. M. De Grand, J. Lee, A. Nakayama, J. A. Parker, T. Mihaljevic, R. G. Laurence, D. M. Dor, *Nat. Biotechnol.* **2003**, *22*, 93; b) Z. Guo, S. Nam, S. Park, J. Yoon, *Chem. Sci.* **2012**, *3*, 2760; c) X. Wu, S. Chang, X. Sun, Z. Guo, Y. Li, J. Tang, Y. Shen, J. Shi, H. Tian, W. Zhu, *Chem. Sci.*, **2013**, *4*, 1221.

[7] J. Yang, J. Choi, D. Bang, E. Kim, E.-K. Lim, H. Park, J.-S. Suh, K. Lee, K.-H. Yoo, E.-K. Kim, Y.-M. Huh, S. Haam, *Angew. Chem Int. Ed.* **2011**, *50*, 441.

[8] a) D. Hertel, H. Marechal, D. A. Tefera, F. Wensheng, R. Hicks, in *Intelligent Vehicles Symposium*, IEEE, **2009**, p 273; b) K. T. Lin, S. C. Tseng, H. L. Chen, Y. S. Lai, S. H. Chen, Y. C. Tseng, T.-W. Chu, M.-Y. Lin, Y.-P. Lu, *J. Mater. Chem. C* **2013**,*1*, 4244.

[9] a) M. Tropiano, N. L. Kilah, M. Morten, H. Rahman, J. J. Davis, P. D. Beer, S. Faulkner, *J. Am. Chem. Soc.* **2011**,*133*, 11847; b) K. Kanazawa, K. Nakamura, N. Kobayashi, *Chem. Commun.* **2011**, *47*, 10064; c) S. Seo, Y. Kim, Q. Zhou, G. Clavier, P. Audebert, E. Kim, *Adv. Funct. Mater.* **2012**, *22*, 3356; d) O. Galangau, I. Fabre-Francke, S. Munteanu, C. Dumas-Verdes, G. Clavier, R. Méallet-Renault, R. B. Pansu, F. Hartl, F. Miomandre, *Electrochim. Acta* **2013**, *87*, 809; e) C. Quinton, V. Alain-Rizzo, C. Dumas-Verdes, F. Miomandre, P. Audebert, *Electrochim. Acta* **2013**, *110*, 693.

[10] a) H. J. Yen, G. S. Liou, *Chem. Commun.* **2013**, *49*, 9797; b) J. H. Wu, G. S. Liou, *Adv. Funct. Mater.* **2014**, *24*, 6406; c) C. P. Kuo, M. K. Leung, *Phys. Chem. Chem. Phys.* **2014**, *16*, 79.

[11] a) A. Beneduci, S. Cospito, M. La Deda, L. Veltri, G. Chidichimo, *Nat. Commun.* **2014**, *5*, 3105, 10.1038/ncomms4105; b) C. Quinton, V. Alain-Rizzo, C. Dumas-Verdes, F. Miomandre, G. Clavier, P. Audebert, *RSC Adv.* **2014**, *4*, 34332; c) K. Kanazawa, K. Nakamura, N. Kobayashi, *J. Phys. Chem. A* **2014**, *118*, 6026.

[12] a) N. Kobayashi, S. Miura, M. Nishimura, Y. Goh, *Electrochim. Acta* **2007**, *53*, 1643; b) S. Cospito, B. C. De Simone, A. Beneduci, D. Imbardelli, G. Chidichimo, *Mater. Chem. Phys.* **2013**, *140*, 431.

[13] a) G. Chidichimo, M. De Benedittis, J. Lanzo, B. C. De Simone, D. Imbardelli, B. Gabriele, L. Veltri, G. Salerno, *Chem. Mater.* **2007**, *19*, 353; b) G. Chidichimo, D. Imbardelli, B. C. De Simone, P. Barone, M. Barberio, A. Bonanno, M. Camarca, A. Oliva, *J. Phys. Chem. C* **2010**, *114*, 16700; c) Chidichimo, B. C. De Simone, D. Imbardelli, M. De Benedittis, M. Barberio, L. Ricciardi, A. Beneduci, *J. Phys. Chem. C* **2014**, *118*, 13484.

[14] a) D. R. Rosseinsky, P. M. S. Monk, *J. Chem. Soc. Faraday Trans.* **1990**, *86*, 3597; b) P. M. S. Monk, R. D. Fairweather, M. D. Ingram, J. A. Duffy, *J. Chem. Soc. Perkin Trans. 2* **1992**, 2039; c) P. M. S. Monk, in *The Viologens*, Wiley, Chichester, UK **1998**; d) D. R. Rosseinsky, R. J. Mortimer, *Adv. Mater.* **2001**, *13*, 783; e) W. W. Porter III, T. P. Vaid, A. L. Rheingold, *J. Am. Chem. Soc.* **2005**, *127*, 16559.

[15] M. E. Alberto, B. C. De Simone, S. Cospito, D. Imbardelli, L. Veltri, G. Chidichimo, N. Russo, *Chem. Phys. Lett.* **2012**, *552*, 141.

[16] a) X. Gu, L. Bi, Y. Fu, N. Wang, S. Liu, Z. Tang, *Chem. Sci.* **2013**, *4*, 4371; b) B. Wang, Y. Ma, S. Wang, L. Zhang, J. Liang, H. Li, L. Wu, L. Bi, *J. Mater. Chem. C* **2014**, *2*, 4423.

[17] Beneduci, S. Cospito, A. Crispini, B. Gabriele, F. P. Nicoletta, L. Veltri, G. Chidichimo , *J. Mater. Chem. C* **2013**, *1*, 2233

[18] a) J. C. de Mello, H. F. Wittmann, R. H. Friend, *Adv. Mater.* **1997**, *9*, 230; b) L. O. Palsonn, A. P. Monkman, *Adv. Mater.* **2002**, *14*, 757; c) L. Porres, A. Holland, L. O. Palsonn, A. P. Monkman, C. Kemp, A. Beeby, *J. Fluorescence* **2006**, *16*, 267.